

## Stable over-expression of PPAR $\beta/\delta$ and PPAR $\gamma$ to examine receptor signaling in human HaCaT keratinocytes

Michael G. Borland <sup>a,b</sup>, Combiz Khozoe <sup>a,1</sup>, Prajakta P. Albrecht <sup>a,1</sup>, Bokai Zhu <sup>a,c</sup>, Christina Lee <sup>a</sup>, Tejas S. Lahoti <sup>a</sup>, Frank J. Gonzalez <sup>d</sup>, Jeffrey M. Peters <sup>a,b,c,\*</sup>

<sup>a</sup> Department of Veterinary and Biomedical Sciences, The Center of Molecular Toxicology and Carcinogenesis, The Pennsylvania State University, University Park, PA 16802, USA

<sup>b</sup> Graduate Program in Biochemistry, Microbiology, and Molecular Biology, The Pennsylvania State University, University Park, PA 16802, USA

<sup>c</sup> The Integrative Biosciences Graduate Program, Huck Institutes for Life Sciences, The Pennsylvania State University, University Park, PA 16802, USA

<sup>d</sup> Laboratory of Metabolism, National Cancer Institute, Bethesda, MD 20892, USA

### ARTICLE INFO

#### Article history:

Received 23 May 2011

Received in revised form 12 July 2011

Accepted 27 July 2011

Available online 4 August 2011

#### Keywords:

Human keratinocytes

PPAR $\beta/\delta$

PPAR $\gamma$

Retinoic acid

Apoptosis

Inflammation

### ABSTRACT

Peroxisome proliferator-activated receptor- $\beta/\delta$  (PPAR $\beta/\delta$ ) function and receptor cross-talk with other nuclear receptors, including PPAR $\gamma$  and retinoic acid receptors (RARs), was examined using stable human HaCaT keratinocyte cell lines over-expressing PPAR $\beta/\delta$  or PPAR $\gamma$ . Enhanced ligand-induced expression of two known PPAR target genes, adipocyte differentiation-related protein (ADRP) and angiopoietin-like protein 4 (ANGPTL4), was found in HaCaT keratinocytes over-expressing PPAR $\beta/\delta$  or PPAR $\gamma$ . Over-expression of PPAR $\beta/\delta$  did not modulate the effect of a PPAR $\gamma$  agonist on up-regulation of ADRP or ANGPTL4 mRNA in HaCaT keratinocytes. All-trans retinoic acid (atRA) increased expression of a known RAR target gene, yet despite a high ratio of fatty acid binding protein 5 (FABP5) to cellular retinoic acid binding protein II, did not increase expression of ANGPTL4 or 3-phosphoinositide-dependent-protein kinase 1 (PDPK1), even in HaCaT keratinocytes expressing markedly higher levels of PPAR $\beta/\delta$ . While PPAR $\beta/\delta$ -dependent attenuation of staurosporine- or UVB-induced poly (ADP-ribose) polymerase (PARP) cleavage was not observed, PPAR $\beta/\delta$ - and PPAR $\gamma$ -dependent repression of UVB-induced expression and secretion of inflammatory cytokines was found in HaCaT keratinocytes over-expressing PPAR $\beta/\delta$  or PPAR $\gamma$ . These studies suggest that FABP5 does not transport atRA or GW0742 to PPAR $\beta/\delta$  and promote anti-apoptotic activity by increasing expression of PDPK1, or that PPAR $\beta/\delta$  interferes with PPAR $\gamma$  transcriptional activity. However, these studies demonstrate that stable over-expression of PPAR $\beta/\delta$  or PPAR $\gamma$  significantly increases the efficacy of ligand activation and represses UVB-induced expression of tumor necrosis factor  $\alpha$  (TNF $\alpha$ ), interleukin 6 (IL6), or IL8 in HaCaT keratinocytes, thereby establishing an excellent model to study the functional role of these receptors in human keratinocytes.

© 2011 Elsevier Inc. All rights reserved.

**Abbreviations:** ADRP, adipocyte differentiation-related protein; atRA, all-trans retinoic acid; ANGPTL4, angiopoietin-like protein 4; CRABP-II, cellular retinoic acid binding protein II; CYP26A1, cytochrome P450 26A1; DMEM, Dulbecco's minimal essential medium; DMSO, dimethylsulfoxide; eGFP, enhanced green fluorescent protein; ELISA, enzyme-linked immunosorbent assay; FABP5, fatty acid binding protein 5; FBS, fetal bovine serum; GAPDH, glyceraldehyde 3-phosphate dehydrogenase; IL6, interleukin 6; IL8, interleukin 8; IRES, internal ribosome entry site; NSAID, non-steroidal anti-inflammatory drug; PDPK1, 3-phosphoinositide-dependent-protein kinase 1; PPAR, peroxisome proliferator-activated receptor; PARP, poly (ADP-ribose) polymerase; qPCR, quantitative real-time polymerase chain reaction; RAR, retinoic acid receptor; RXR, retinoid X receptor; TNF $\alpha$ , tumor necrosis factor  $\alpha$ ; UVB, ultraviolet B.

\* Corresponding author at: Department of Veterinary and Biomedical Sciences, The Pennsylvania State University, 312 Life Science Building, University Park, PA 16802, USA. Tel.: +1 814 863 1387; fax: +1 814 863 1696.

E-mail address: [jmp21@psu.edu](mailto:jmp21@psu.edu) (J.M. Peters).

<sup>1</sup> Equally contributing authors.

### 1. Introduction

It is firmly established that ligand activation of peroxisome proliferator-activated receptor- $\beta/\delta$  (PPAR $\beta/\delta$ ) can increase lipid catabolism in skeletal muscle [1], reduce serum lipids levels [2], increase serum high density lipoprotein cholesterol [2,3], improve glucose intolerance observed with dietary-induced obesity [1,4], promote terminal differentiation (reviewed in [5,6]), and lead to a variety of anti-inflammatory activities (reviewed in [3]). However, there are a number of examples where conflicting literature exists that prevents a more definitive understanding of PPAR $\beta/\delta$  function (reviewed in [4,5]). Given the potential of targeting this nuclear receptor for the treatment and prevention of disease, there is a distinct need to delineate whether PPAR $\beta/\delta$  can, or cannot, be targeted by small molecules for these purposes due to possible safety issues. Toward this goal, the generation of knockout and knockdown models [9–11] and the development of highly specific agonists and

antagonists [6] have proven of great value for investigating the potential for targeting PPAR $\beta/\delta$  for drug development.

Expression of PPAR $\beta/\delta$  is markedly higher in intestine and keratinocytes as compared to many other tissues in both humans and mice [7,8]. PPAR $\beta/\delta$  is found predominantly in the nucleus and can be co-immunoprecipitated with its heterodimerization partner, retinoid X receptor (RXR) [7]. This suggests that PPAR $\beta/\delta$  has an intrinsic, constitutive function. Consistent with this idea, genetic disruption of PPAR $\beta/\delta$  revealed that PPAR $\beta/\delta$  inhibits epithelial cell proliferation [10,18]. Three different *Ppar* $\beta/\delta$ -null mouse models using three different targeting approaches have been produced [9,10,19], and used to elucidate the developmental and physiological functions of PPAR $\beta/\delta$ . The phenotypes of the three different *Ppar* $\beta/\delta$ -null mouse models differ in some cases but are concordant for others. For example, genetic disruption of PPAR $\beta/\delta$  caused enhanced phorbol ester-induced epithelial hyperplasia in two different models [9]. In contrast, when *Ppar* $\beta/\delta$ -null mice were crossed with APC<sup>min</sup> heterozygous mice, one model exhibited no change in colon carcinogenesis [10], one model exhibited increased colon tumorigenesis [21,22], and another model exhibited decreased colon tumorigenesis [11]. This illustrates the need for alternative approaches and/or models to study the functional role of PPAR $\beta/\delta$ .

In addition to null mouse models, the development of highly specific PPAR $\beta/\delta$  ligands has also been instrumental for evaluating the effects of PPAR $\beta/\delta$  activation, in particular when coupled with *Ppar* $\beta/\delta$ -null mouse models. For example, GW501516 selectively activates human PPAR $\beta/\delta$  with close to 1000-fold greater affinity as compared to human PPAR $\alpha$  or PPAR $\gamma$  based on in vitro reporter assays [12]. However, this selectivity is greatly reduced for mouse PPARs where GW501516 only exhibits  $\leq 62$ -fold greater affinity for PPAR $\beta/\delta$  as compared to PPAR $\alpha$  or PPAR $\gamma$  [12]. This difference in ligand selectivity between species illustrates the need for controls including knockout/knockdown and/or over-expression models in order to demonstrate specificity. Collectively, despite the current availability of null mouse models and high affinity ligands with specificity toward PPAR $\beta/\delta$ , there remains a need for alternative approaches to study the role of PPAR $\beta/\delta$ , as evidenced by the conflicting literature that exists preventing a more definitive understanding of PPAR $\beta/\delta$  function (reviewed in [4,5]). For these reasons, the present study characterized a new human keratinocyte model where PPAR $\beta/\delta$  is over-expressed to provide a new tool for elucidating the role of PPAR $\beta/\delta$  in cell proliferation and carcinogenesis.

## 2. Materials and methods

### 2.1. Materials and cell culture

[4-[[[2-[3-fluoro-4-(trifluoromethyl)phenyl]-4-methyl-5-thiazolyl]methyl]thio]-2-methylphenoxy acetic acid (GW0742) was synthesized by GlaxoSmithKline (Research Triangle Park, NC) [13]. All-trans retinoic acid (atRA) was purchased (Sigma Aldrich, St. Louis, MO). GW0742 was dissolved in dimethylsulfoxide (DMSO) and atRA was dissolved in ethanol. The pMigr1 vector (Migr1) and p $\psi$ -Ampho have been previously described [14]. Briefly, the Migr1 retroviral vector encodes the murine stem cell virus promoter that drives expression of cDNA cloned into a cloning site, followed by an internal ribosome entry site (IRES) and a sequence encoding enhanced green fluorescent protein (eGFP) [14]. This vector allows for expression of a protein of interest and eGFP, which facilitates identification and sorting of cells that have stably integrated the Migr1 retroviral vector. The pcDNA3.1-hPPAR $\beta/\delta$  and pcDNA3.1-hPPAR $\gamma$  constructs were kindly provided by Dr. Curtis Omiecinski (The Pennsylvania State University, University Park, PA). Primers for quantitative real-time polymerase chain reaction (qPCR) were purchased from Integrated DNA Technologies (IDT, Coralville, IA). HaCaT cells were kindly provided by Dr. Stuart Yuspa (National Cancer Institute, Bethesda, MD), and HEK293T cells were kindly provided by Dr. Yanming Wang (The Pennsylvania State University, University Park,

PA). Both cell lines were cultured in Dulbecco's minimal essential medium (DMEM) supplemented with 10% fetal bovine serum (FBS) and 1% penicillin/streptomycin at 37 °C and 5% CO<sub>2</sub>.

### 2.2. Establishment of Migr1 stable cell lines

The Migr1-hPPAR $\beta/\delta$  and Migr1-hPPAR $\gamma$  vectors were created by subcloning the human PPAR $\beta/\delta$  and PPAR $\gamma$  cDNA sequences from pcDNA3.1-hPPAR $\beta/\delta$  and pcDNA3.1-hPPAR $\gamma$  into the Migr1 vector. The coding sequence of all constructs was confirmed by sequencing at the Penn State University Nucleic Acid Facility. Stable Migr1 (vector control), Migr1-hPPAR $\beta/\delta$ , and Migr1-hPPAR $\gamma$  cell lines were established by retrovirus spinoculation as previously described [14]. Briefly, each construct and p $\psi$ -Ampho plasmids were co-transfected into HEK293T cells to produce retrovirus using the Lipofectamine® transfection reagent and the manufacturer's recommended protocol. Forty-eight hours after transfection, the supernatant containing the retrovirus was filtered with a 0.22  $\mu$ m filter and used to spinoculate HaCaT cells. eGFP-positive cells were isolated by fluorescence-activated cell sorting using an InFlux V-GS Cytometry Workbench and the Spigot software (BD Biosciences, San Jose, CA). Forward-scatter and side-scatter dot plots gave the cellular physical properties of size and granularity and allowed gating for live cells. Fluorescence was excited at 488 nm, and emission was collected using a 525 nm (eGFP) band-pass filter. Collected eGFP cells possessed a minimum of 100-fold higher eGFP expression than non-eGFP cells. Fluorescence photomicrographs were obtained with a SPOT SP100 cooled CCD camera fitted to a Nikon Eclipse TE300 upright microscope with EFD-3 episcopic fluorescence attachment. The presence of eGFP fluorescence was routinely checked using the Nikon fluorescence microscope.

### 2.3. Characterization of the Migr1 over-expression models

Western blot analysis was performed as described below to verify that the PPARs were over-expressed. The ability of the different cell lines to respond to ligand activation was examined by treating cells with different agonists. Ligand activation of PPAR $\beta/\delta$  was examined in HaCaT keratinocytes, HaCaT-Migr1 vector control cells, and HaCaT-Migr1-hPPAR $\beta/\delta$  cells cultured in medium with vehicle (0.02% DMSO) or the PPAR $\beta/\delta$  ligand GW0742 (0.01–10  $\mu$ M) for 8 h. Ligand activation of PPAR $\gamma$  was examined in HaCaT keratinocytes, HaCaT-Migr1 vector control cells, and HaCaT-Migr1-hPPAR $\gamma$  cells cultured in medium with vehicle (0.02% DMSO) or the PPAR $\gamma$  ligand rosiglitazone (0.01–10  $\mu$ M) for 24 h. Analysis of gene expression was performed as described below.

### 2.4. Examination of putative receptor cross-talk

It was previously suggested by others that the ratio of fatty acid binding protein 5 (FABP5) to cellular retinoic acid binding protein II (CRABP-II) determines whether atRA or PPAR $\beta/\delta$  ligands activate either PPAR $\beta/\delta$  or RAR and modulate cell survival by increased expression of 3-phosphoinositide-dependent-protein kinase 1 (PDPK1) [15]. In this hypothetical model, PPAR $\beta/\delta$  is activated by atRA or PPAR $\beta/\delta$  ligands in cells where expression of FABP5 is high as compared to expression of CRABP-II due to preferential delivery of ligands via FABP5 rather than CRABP-II. This hypothesis was based in part on data obtained from HaCaT keratinocytes that exhibit a relatively high FABP5/CRABP-II ratio. This suggests that if PPAR $\beta/\delta$  expression was increased, then the ability of atRA to activate PPAR $\beta/\delta$  and modulate expression of PPAR $\beta/\delta$  target genes or PDPK1 should increase. This hypothesis was examined in greater detail in HaCaT keratinocytes, HaCaT-Migr1 vector control cells, and HaCaT-Migr1-hPPAR $\beta/\delta$  cells. Western blot analysis was performed to quantify relative expression of FABP5 and CRABP-II as described below. Cells were cultured in medium with vehicle (0.1% ethanol) or atRA (0.1 and 1.0  $\mu$ M) for 8 to 16 h and expression of PDPK1, the RAR target gene cytochrome P450 26A1 (*CYP26A1*), and the PPAR target genes adipocyte differentiation-related protein (*ADRP*) and angiopoietin-like protein 4

(*ANGPTL4*) was determined by qPCR and/or western blot analysis as described below.

As it was suggested that PPAR $\beta/\delta$  can interfere with PPAR $\gamma$ -dependent transcription [27,28], this idea was examined in HaCaT keratinocytes, HaCaT-Migr1 vector control cells, HaCaT-Migr1-hPPAR $\beta/\delta$  cells, and HaCaT-Migr1-hPPAR $\gamma$  cells cultured in medium with vehicle (DMSO), GW0742 (0.1 or 1.0  $\mu$ M) or rosiglitazone (1 or 10  $\mu$ M) for 8 or 24 h, respectively. *ADRP* and *ANGPTL4* mRNA was measured because expression can be increased by activating either PPAR $\beta/\delta$  or PPAR $\gamma$  due to PPAR response elements located near these genes [16–18].

### 2.5. Western blot analysis

Soluble protein lysates were isolated from 90 to 95% confluent 100 mm culture dishes using a modified MENG buffer (25 mM MOPS, 2 mM EDTA, 0.02% Na<sub>3</sub>, and 10% glycerol, pH 7.5) containing 500 mM NaCl, 1% Nonidet P-40, and protease inhibitors. Fifty micrograms of protein per sample was resolved using SDS-polyacrylamide gels and transferred to a nitrocellulose membrane using an electroblotting method. The membranes were blocked with 5% dried milk in Tris buffered saline/Tween-20 and incubated overnight with primary antibodies. After incubation with biotinylated secondary antibody (Jackson ImmunoResearch Laboratories, West Grove, PA), immunoreactive proteins were detected after incubation with <sup>125</sup>I-streptavidin. Membranes were exposed to plates and the level of radioactivity quantified with filmless autoradiographic analysis. Hybridization signals for specific proteins were normalized to the hybridization signal for lactate dehydrogenase (LDH) or ACTIN. The following antibodies were used: anti-LDH or anti-ACTIN (Rockland, Gilbertsville, PA), anti-human PPAR $\beta/\delta$  (ab21209, Abcam, Cambridge, MA), anti-human PPAR $\gamma$  (2430, Cell Signaling Technology, Danvers, MA), anti-PDPK1 (611070, BD Biosciences, San Diego, CA), anti-CYP26A1 (AB64888, Abcam, Cambridge, MA), anti-human CRABP-II (ab74365-100, Abcam, Cambridge, MA), anti-human FABP5 (RD181060100, BioVendor, Chandler, NC), anti-RXR $\alpha$  (SC553, Santa Cruz Biotechnology, Santa Cruz, CA) or anti-PARP (9542, Cell Signaling Technology, Danvers, MA).

### 2.6. Quantitative real-time polymerase chain reaction (qPCR)

Total RNA was isolated from cells using RiboZol RNA Extraction Reagent (AMRESCO, Solon, OH) and the manufacturer's recommended protocol. The mRNA encoding *ANGPTL4*, *CYP26A1*, *PDPK1* and glyceraldehyde 3-phosphate dehydrogenase (*GAPDH*) was measured by qPCR analysis using the previously described primers [19]. The mRNA encoding *ADRP* (NM\_001122) was measured by qPCR analysis using the following primers: forward 5'-CTGCTCTTCGCTTTCGCT-3' and reverse 5'-ACCACCGAGTACCACACT-3'. cDNA was generated from 1.25  $\mu$ g of total RNA using MultiScribe Reverse Transcriptase kit (Applied Biosystems, Foster City, CA). The quantitative real-time PCR analysis was carried out using SYBR<sup>®</sup> Green PCR Supermix for IQ (Quanta Biosciences, Gaithersburg, MD) in the iCycler and detected using the MyiQ Realtime PCR Detection System (Bio-Rad Laboratories, Hercules, CA). The following PCR reaction was used for all mRNAs: 95 °C for 10 s, 60 °C for 30 s, and 72 °C for 30 s, repeated for 45 cycles. Each PCR reaction included a no-template control reaction to control for contamination, and all real-time PCR reactions had greater than 85% efficiency. The relative mRNA value for each gene was normalized to the relative mRNA value for the housekeeping gene *GAPDH*.

### 2.7. Flow cytometry of cell cycle

HaCaT keratinocytes were seeded onto 6-well tissue culture dishes at a concentration of 250,000 cells per well and cultured in DMEM (with 10% FBS and 1% penicillin/streptomycin). Twenty-four hours after plating, cells were treated with GW0742 (0.01, 0.1, 1.0 or 10  $\mu$ M) or

rosiglitazone (0.01, 0.1, 1.0, 10.0 or 25.0  $\mu$ M) for 24 h. After these treatments, culture medium was removed and the cells were trypsinized. Trypsinized cells were pelleted and fixed in ice cold 70% ethanol. Prior to analysis, cells were stained with propidium iodide (PI) solution containing 1  $\mu$ g PI/ $\mu$ L and 0.125% RNase A (Sigma Aldrich, St. Louis, MO). Approximately 10,000 cells/sample were analyzed using an EPICS-XL-MCL flow cytometer (Beckman Coulter, Miami Lakes, FL) fitted with a single 15-mW argon ion laser providing excitation at 488 nm. The percentage of cells at each phase of the cell cycle was determined with MultiCycle<sup>®</sup> analysis software. Values were calculated from a minimum of three independent samples per treatment.

### 2.8. Effect of PPAR $\beta/\delta$ and PPAR $\gamma$ on modulation of apoptotic signaling

While it is generally accepted that PPAR $\gamma$  can in some instances promote apoptosis, the role of PPAR $\beta/\delta$  in apoptotic signaling is confusing because there are studies showing that PPAR $\beta/\delta$  either, promotes, attenuates, or has no effect on apoptotic signaling (reviewed in [5]). Thus, the effect of PPAR $\beta/\delta$  and PPAR $\gamma$  on modulation of staurosporine-induced or ultraviolet B (UVB)-induced PARP cleavage, as a measure of apoptotic signaling, was examined. To determine the temporal changes of PARP cleavage, HaCaT keratinocytes, HaCaT-Migr1 vector control cells, HaCaT-Migr1-hPPAR $\beta/\delta$  cells or HaCaT-Migr1-hPPAR $\gamma$  cells were cultured until 90–95% confluent, and then treated with either 0.5  $\mu$ M staurosporine or irradiated with UVB (280–315 nm, 50 mJ/cm<sup>2</sup>) in phosphate buffered saline (PBS) using a CL-1000 Ultraviolet Crosslinker (Ultra-Violet Products, Inc., Upland, CA). Protein was isolated from cells at 0, 0.5, 1, 2 or 4 hour post-staurosporine treatment or 0, 1, 2, 4 or 8 hour post-UVB irradiation. To determine the effect of ligand activation of PPAR $\beta/\delta$  or PPAR $\gamma$  on staurosporine-induced or UVB-induced PARP cleavage, cells were cultured in medium with or without GW0742 (0, 0.1 or 1.0  $\mu$ M) or rosiglitazone (0, 1 or 10  $\mu$ M) for 1 h prior to irradiation or staurosporine treatment, and then cultured in medium with or without GW0742 or rosiglitazone. Protein was isolated from cells at 0, 1 or 2 hour post-staurosporine treatment or 0, 4 or 8 hour post-UVB treatment. Western blot analysis was performed as described above to quantify PARP cleavage.

### 2.9. Effect of PPAR $\beta/\delta$ and PPAR $\gamma$ on modulation of UVB-induced inflammation

The effect of PPAR $\beta/\delta$  and PPAR $\gamma$  on modulation of UVB-induced expression of inflammatory cytokines was examined in HaCaT keratinocytes, HaCaT-Migr1 vector control cells, HaCaT-Migr1-hPPAR $\beta/\delta$  cells or HaCaT-Migr1-hPPAR $\gamma$  cells. To determine the temporal changes of pro-inflammatory cytokine mRNA expression, 90–95% confluent cells were irradiated as described above. RNA was isolated from cells at 0, 1, 2, 4 or 8 hour post-irradiation. To determine the effect of ligand activation of PPAR $\beta/\delta$  or PPAR $\gamma$  on pro-inflammatory cytokine mRNA expression, cells were cultured in medium with or without GW0742 (0, 0.1 or 1.0  $\mu$ M) or rosiglitazone (0, 1 or 10  $\mu$ M) for 1 h prior to irradiation, and then cultured in medium with or without GW0742 or rosiglitazone for 4 h. Total RNA was isolated and qPCR analysis was performed as described above to quantify expression of mRNA encoding *IL6*, interleukin 8 (*IL8*) and *TNF $\alpha$* . The following primers were used: human *IL6* (NM\_000600) forward: 5'-AAATTCGGTACATCCTC-GACGGCA-3', reverse: 5'-AGTGCCTCTTTGCTGCTTTACAC-3'; human *IL8* (NM\_000582) forward: 5'-AGCCTTCCTGATTCTGCAGCTCT-3', reverse: 5'-AATTTCTGTGTTGGCGAGTGTGG-3'; human *TNF $\alpha$*  (NM\_000594) forward: 5'-ACCCACGGCTCCACCCTCTC-3', reverse: 5'-AGGTCCTGGG-GAACTCTTCCT-3'.

### 2.10. Enzyme-linked immunosorbent assay (ELISA)

ELISAs were performed to quantify the concentration of tumor necrosis factor  $\alpha$  (TNF $\alpha$ ) and interleukin 6 (IL6), in culture medium

using commercially available kits (TNF $\alpha$  kit was purchased from R&D Systems, Minneapolis, MN; IL6 kit was purchased from Biolegend, San Diego, CA).

### 2.11. Data analysis

Data were analyzed for statistical significance using one-way analysis of variance (ANOVA) and the Bonferroni's multiple comparison tests, or Student's *T*-test as described in the figure legends. All data are

presented as the mean  $\pm$  standard error of the mean (SEM) using Prism 5.0 (GraphPad Software Inc., La Jolla, CA).

## 3. Results

### 3.1. Enhanced receptor activity in HaCaT keratinocyte over-expressing PPAR $\beta/\delta$ or PPAR $\gamma$

The Migr1 retroviral system [14] was used to generate HaCaT cells over-expressing PPAR $\beta/\delta$  and PPAR $\gamma$  for gain-of-function models to

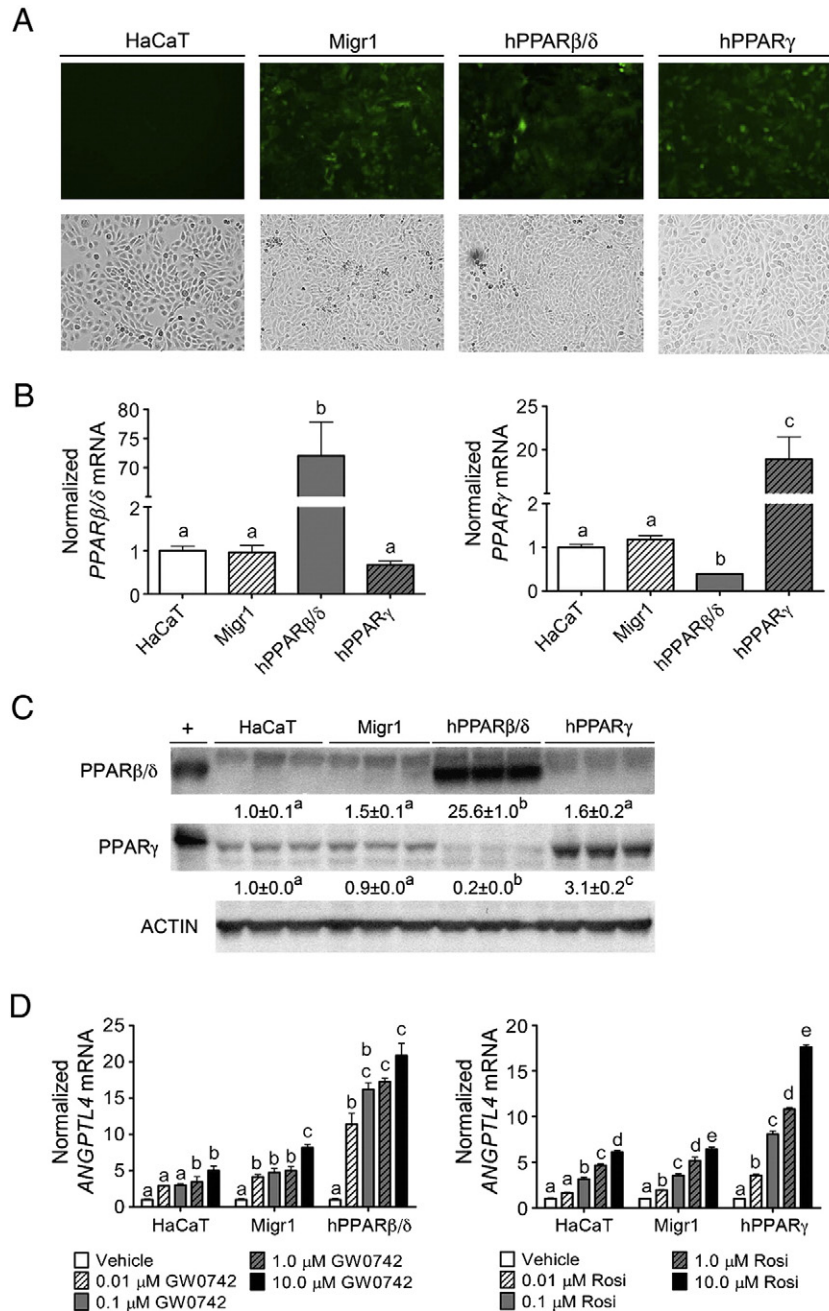


**Fig. 1.** Characterization of Migr1 over-expression of PPAR $\beta/\delta$  and PPAR $\gamma$ . HaCaT cells were infected with empty vector (Migr1), hPPAR $\beta/\delta$ , or hPPAR $\gamma$ , and stable GFP positive cells were sorted by flow cytometry and propagated as described in [Materials and methods](#). (A) GFP fluorescence of sorted HaCaT keratinocytes, HaCaT-Migr1 vector control cells (Migr1), HaCaT-Migr1-hPPAR $\beta/\delta$  cells (hPPAR $\beta/\delta$ ) and HaCaT-Migr1-hPPAR $\gamma$  cells (hPPAR $\gamma$ ). (B) mRNA expression of PPAR $\beta/\delta$  and PPAR $\gamma$  in the Migr1 cell lines as compared to HaCaT keratinocytes. qPCR was performed to examine the expression of mRNA encoding PPAR $\beta/\delta$  and PPAR $\gamma$ . (C) Protein expression of PPAR $\beta/\delta$  and PPAR $\gamma$  was assessed by Western blotting in the Migr1 cell lines as compared to HaCaT keratinocytes. (D) Ligand response of HaCaT cell lines to the PPAR $\beta/\delta$  ligand GW0742 for 8 h and the PPAR $\gamma$  ligand rosiglitazone for 24 h. qPCR was performed to examine the expression of the mRNA encoding *ANGPTL4* normalized to the mRNA encoding *GAPDH*. Fold induction of *ANGPTL4* mRNA was calculated by normalization to vehicle control for each cell line. Data represents triplicate independent sample means  $\pm$  SEM. Values with different letters are significantly different ( $P \leq 0.05$ ) using Bonferroni's multiple comparison.

study PPAR signaling in human keratinocytes. After eGFP sorting and propagation of heterogeneous cell populations, stable cell lines were characterized for eGFP fluorescence, PPAR protein expression, and ligand-dependent transcriptional regulation. HaCaT-Migr1 vector control, HaCaT-Migr1-hPPAR $\beta/\delta$ , and HaCaT-Migr1-hPPAR $\gamma$  cells exhibited strong eGFP fluorescence that was not observed in control, uninfected HaCaT keratinocytes (Fig. 1A). No macroscopic changes in cell morphology were observed in any of these cell lines as compared to the parent HaCaT keratinocytes (Fig. 1A). Stable integration of the expression constructs for PPAR-specific proteins led to increased PPAR $\beta/\delta$  or PPAR $\gamma$  mRNA in respective cell lines as compared to controls (Fig. 1B). Interestingly, expression of PPAR $\gamma$  mRNA was lower in HaCaT-Migr1-hPPAR $\beta/\delta$  cells as compared to controls (Fig. 1B). A marked increase of PPAR $\beta/\delta$  protein was found in HaCaT keratinocytes infected with Migr1-hPPAR $\beta/\delta$  as compared to HaCaT-Migr1 vector control cells and the control HaCaT keratinocytes (Fig. 1C). Increased expression of PPAR $\gamma$  protein was found in HaCaT keratinocytes infected with Migr1-hPPAR $\gamma$  as compared to HaCaT-Migr1 vector control cells and the parent HaCaT keratinocytes (Fig. 1C). Consistent with the observed decrease in mRNA encoding PPAR $\gamma$  mRNA, expression of PPAR $\gamma$  protein was also relatively lower in HaCaT-Migr1-hPPAR $\beta/\delta$  cells as compared to controls (Fig. 1C). To determine whether the increase in expression of PPARs led to functional changes in their ability to modulate ligand-dependent transcriptional regulation, the effect of ligand activation was examined using the high affinity PPAR $\beta/\delta$  ligand, GW0742, or the PPAR $\gamma$  ligand, rosiglitazone. The target gene *ANGPTL4* was used for this analysis as expression of this gene can be increased by ligand activation of both PPAR $\beta/\delta$  or PPAR $\gamma$ , depending on expression of receptor and the presence of specific ligands [18]. A dose dependent increase in expression of *ANGPTL4* mRNA was observed in parent HaCaT keratinocytes and HaCaT-Migr1 vector control cells in response to 0.01  $\mu$ M to 10  $\mu$ M GW0742

(Fig. 1D). Markedly higher increases in ligand induced expression of *ANGPTL4* mRNA was observed in HaCaT-Migr1-hPPAR $\beta/\delta$  cells in response to 0.01  $\mu$ M to 10  $\mu$ M GW0742 as compared to both parent HaCaT keratinocytes and HaCaT-Migr1 vector control cells (Fig. 1D). Similarly, a dose dependent increase in expression of *ANGPTL4* mRNA was observed in parent HaCaT keratinocytes and HaCaT-Migr1 vector control cells in response to 0.01  $\mu$ M to 10  $\mu$ M rosiglitazone (Fig. 1D). Additionally, higher increases in ligand induced expression of *ANGPTL4* mRNA were observed in HaCaT-Migr1-hPPAR $\gamma$  cells in response to 0.01  $\mu$ M to 10  $\mu$ M rosiglitazone as compared to both control HaCaT keratinocytes and HaCaT-Migr1 vector control cells (Fig. 1D). It is also worth noting that a significant difference in ligand-induced expression of *ANGPTL4* mRNA was not observed between the parent HaCaT keratinocyte cell line and the Migr1 vector control cell lines (Fig. 1D). Combined, these data establish that over-expression of PPAR $\beta/\delta$  or PPAR $\gamma$  in HaCaT keratinocytes can cause enhanced ligand-induced receptor activity and provides a useful model for examining the functional roles of these receptors.

### 3.2. Over-expression of PPAR $\beta/\delta$ does not interfere with PPAR $\gamma$ activity in HaCaT keratinocytes

Previous in vitro studies suggest that PPAR $\beta/\delta$  can interfere or inhibit PPAR $\gamma$ -dependent gene expression [27,28]. However, these studies are limited since this idea was based on examination of reporter assays and limited analysis ( $n = 1$ ) of an endogenous target gene [27,28]. Thus, the effect of ligand activation of PPAR $\beta/\delta$  or PPAR $\gamma$  on expression of two well-characterized PPAR target genes (*ADRP* and *ANGPTL4*) was examined in HaCaT keratinocytes over-expressing PPAR $\beta/\delta$  or PPAR $\gamma$  by direct comparison in the same experiment. A dose-dependent increase in expression of *ANGPTL4* and *ADRP* mRNA was found in parent HaCaT keratinocytes, HaCaT-Migr1 vector control cells, and HaCaT-

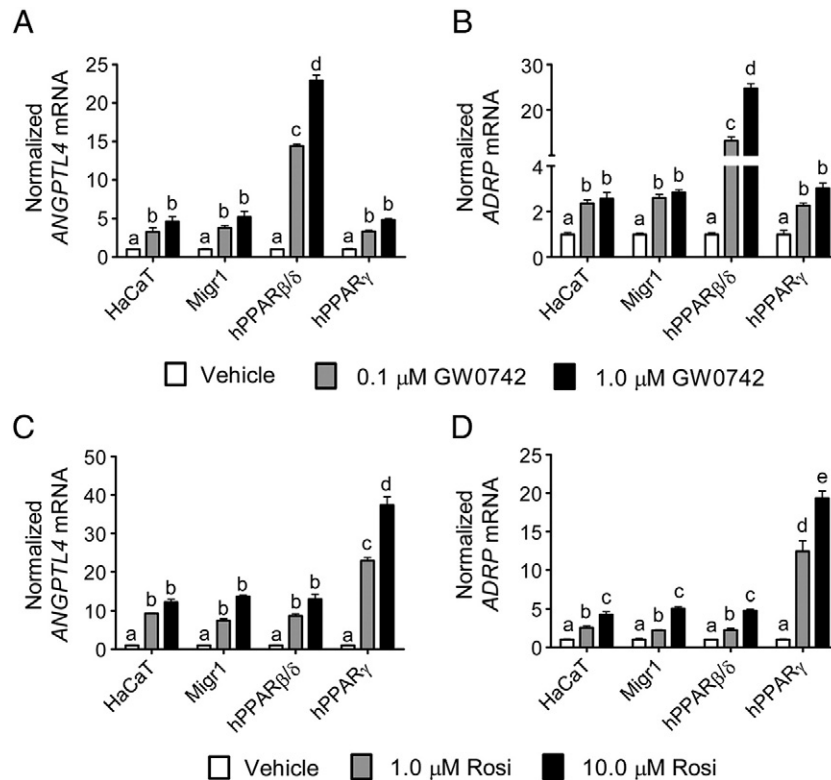


**Fig. 2.** Effect of modulated PPAR $\beta/\delta$  and PPAR $\gamma$  expression on receptor-dependent transcriptional regulation. Quantitative real-time PCR (qPCR) for *ANGPTL4* and *ADRP* mRNA in HaCaT keratinocytes, HaCaT-Migr1 vector control cells (Migr1), HaCaT-Migr1-hPPAR $\beta/\delta$  cells (hPPAR $\beta/\delta$ ) and HaCaT-Migr1-hPPAR $\gamma$  cells (hPPAR $\gamma$ ) treated with the PPAR $\beta/\delta$  ligand GW0742 for 8 h (A,B) or the PPAR $\gamma$  rosiglitazone (Rosi) for 24 h (C,D). mRNA was isolated from the cells following indicated treatments and qPCR was performed to examine the expression of the mRNA encoding *ANGPTL4* and *ADRP*, as normalized to the mRNA encoding *GAPDH*. Fold induction of *ANGPTL4* and *ADRP* mRNA was calculated by normalization to vehicle control for each cell line. Data represents triplicate independent sample means  $\pm$  SEM. Values with different letters are significantly different ( $P \leq 0.05$ ) using Bonferroni's multiple comparison.

Migr1-hPPAR $\gamma$  cells in response to 0.1 and 1.0  $\mu$ M GW0742, and this increase in expression was similar between these three cell lines (Fig. 2A,B). In HaCaT-Migr1-hPPAR $\beta/\delta$  cells, ligand activation of PPAR $\beta/\delta$  with GW0742 resulted in a dose-dependent increase in *ANGPTL4* and *ADRP* mRNA that was markedly greater as compared to the effect of ligand in parent HaCaT keratinocytes, HaCaT-Migr1 vector control cells, and HaCaT-Migr1-hPPAR $\gamma$  cells (Fig. 2A,B). Similarly, increased expression of *ANGPTL4* and *ADRP* mRNA was found in parent HaCaT keratinocytes, HaCaT-Migr1 vector control cells, and HaCaT-Migr1-hPPAR $\beta/\delta$  cells in response to 1.0 and 10.0  $\mu$ M rosiglitazone, and this increase in expression was similar between these three cell lines (Fig. 2C,D). In HaCaT-Migr1-hPPAR $\gamma$  cells, ligand activation of PPAR $\gamma$  with rosiglitazone resulted in a marked increase in *ANGPTL4* and *ADRP* mRNA as compared to the parent HaCaT keratinocytes, HaCaT-Migr1 vector control cells and HaCaT-Migr1-hPPAR $\beta/\delta$  cells (Fig. 2C,D). While the relative expression of PPAR $\gamma$  was lower in HaCaT-Migr1-hPPAR $\beta/\delta$  cells as compared to controls (Fig. 1B,C), this change was not reflected in the ability of rosiglitazone to activate PPAR $\gamma$  target gene expression as the efficacy of *ANGPTL4* and *ADRP* mRNA induction by rosiglitazone was

comparable between the parent HaCaT keratinocytes, HaCaT-Migr1 vector control cells and HaCaT-Migr1-hPPAR $\beta/\delta$  cells (Fig. 2C,D).

### 3.3. Over-expression of PPAR $\beta/\delta$ does not increase FABP5 shuttling of atRA or PPAR $\beta/\delta$ ligands to PPAR $\beta/\delta$

It was suggested that the biological effects of atRA or PPAR $\beta/\delta$  ligands could be modulated by differential shuttling of atRA or PPAR $\beta/\delta$  ligands between RAR and PPAR $\beta/\delta$  [15]. In this hypothetical model, shuttling of atRA toward RAR occurs in cells expressing more cellular retinoic acid binding protein II (CRABP-II) as compared to fatty acid binding protein 5 (FABP5), whereas atRA (or PPAR $\beta/\delta$  ligands) is shuttled toward PPAR $\beta/\delta$  in cells expressing more FABP5 as compared to CRABP-II leading to activation of PPAR $\beta/\delta$ , increased expression of target genes and PDPK1, and increased cell survival [15]. Expression of FABP5 was approximately 5–6 $\times$  higher as compared to CRABP-II in parent HaCaT keratinocytes, HaCaT-Migr1 vector control cells, and HaCaT-Migr1-hPPAR $\beta/\delta$  cells (Fig. 3A). Expression of PPAR $\beta/\delta$  was more than 5–6 $\times$  higher in HaCaT-Migr1-hPPAR $\beta/\delta$  as compared to parent HaCaT keratinocytes and HaCaT-

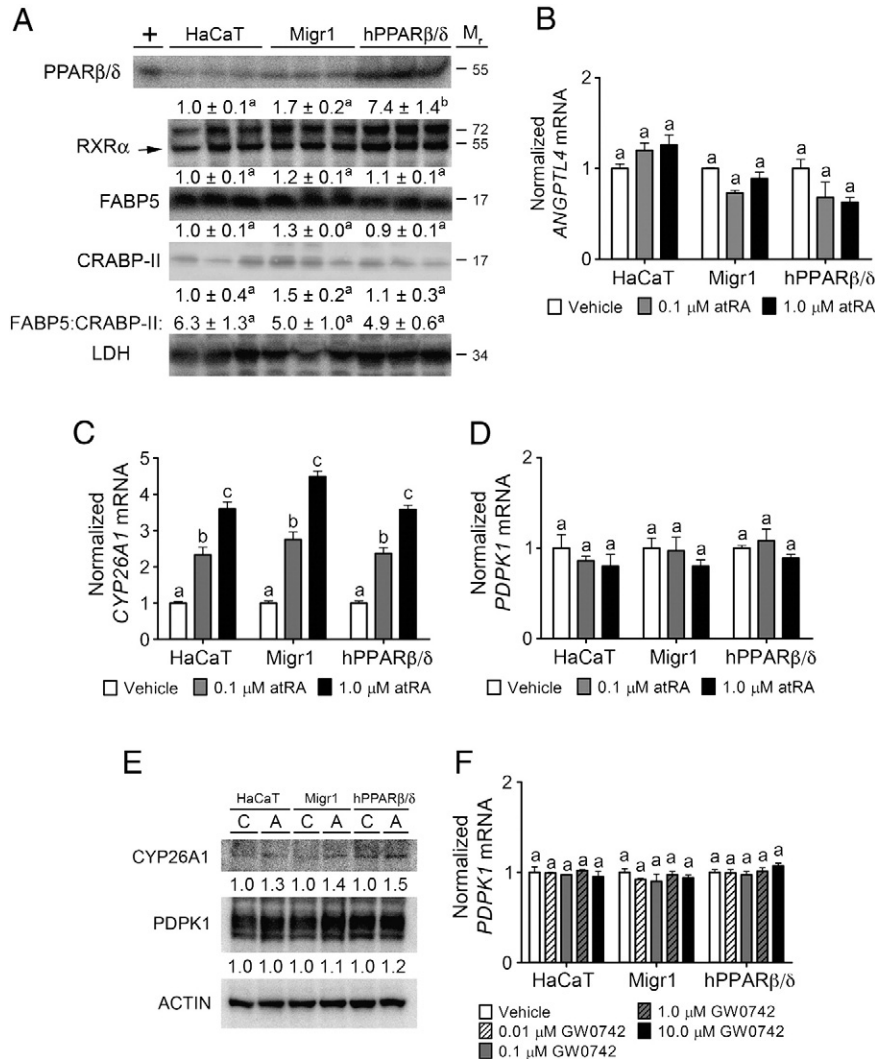


**Fig. 3.** Effect of modulated PPAR $\beta/\delta$  expression on retinoic acid signaling. (A) Western blot analysis of PPAR $\beta/\delta$ , RXR $\alpha$ , FABP5 and CRABP-II. Lysates from HaCaT keratinocytes, HaCaT-Migr1 vector control cells (Migr1) or HaCaT-Migr1-hPPAR $\beta/\delta$  cells (hPPAR $\beta/\delta$ ) were prepared and probed for PPAR $\beta/\delta$ , RXR $\alpha$ , FABP5, CRABP-II, and LDH expression. Cells were treated with retinoic acid for 8 h and qPCR was performed to quantify mRNAs for the (B) PPAR $\beta/\delta$ -dependent target gene *ANGPTL4*, (C) the RAR-dependent target gene *CYP26A1*, and (D) the putative PPAR $\beta/\delta$ -dependent target gene *PDPK1*. Fold induction of mRNA was calculated from data normalized to *GAPDH* mRNA relative to vehicle control for each cell line. (E) Cells were treated with retinoic acid (1.0  $\mu$ M) for 16 h and western blot analysis was performed to quantify expression of *CYP26A1* or *PDPK1*. (F) *PDPK1* mRNA expression in cells following ligand activation of PPAR $\beta/\delta$  with GW0742 for 8 h. Data represents triplicate independent sample means  $\pm$  SEM (A–D,F). Values with different letters are significantly different ( $P \leq 0.05$ ) using Bonferroni's multiple comparison.

Migr1 vector control cells (Fig. 3A). Expression of RXR $\alpha$  was similar in HaCaT keratinocytes, HaCaT-Migr1 vector control cells, and HaCaT-Migr1-hPPAR $\beta/\delta$  cells (Fig. 3A). HaCaT keratinocytes, HaCaT-Migr1 vector control cells, and HaCaT-Migr1-hPPAR $\beta/\delta$  cells cultured in the presence of atRA exhibited no change in expression of the PPAR target gene *ANGPTL4* (Fig. 3B), while comparable dose dependent increases in mRNA expression of the RAR target gene *CYP26A1* was observed in all three cell lines (Fig. 3C). The change in *CYP26A1* mRNA was confirmed at the protein level by western blot analysis (Fig. 3E). Expression of *PDPK1* mRNA or protein was unchanged in response to atRA (Fig. 3D,E) in HaCaT keratinocytes, HaCaT-Migr1 vector control cells, and HaCaT-Migr1-hPPAR $\beta/\delta$  cells. Further, expression of *PDPK1* mRNA was unchanged in response GW0742 (Fig. 3F) in HaCaT keratinocytes, HaCaT-Migr1 vector control cells, and HaCaT-Migr1-hPPAR $\beta/\delta$  cells. Thus, despite over-expression of functional PPAR $\beta/\delta$  in cells expressing a high FABP5 to CRABP-II ratio, increased shuttling of atRA or the PPAR $\beta/\delta$  ligand GW0742 toward PPAR $\beta/\delta$  was not observed.

#### 3.4. Effect of over-expression of PPAR $\beta/\delta$ and PPAR $\gamma$ on cell cycle progression in HaCaT keratinocytes

In response to ligand activation of PPAR $\beta/\delta$  or PPAR $\gamma$ , HaCaT keratinocytes or human keratinocytes exhibit modest inhibition of cell proliferation mediated in part by a small increase in apoptosis [19,20], but these effects are not as strong as compared to more potent inhibitors of cell proliferation such as ultraviolet radiation [21]. However, it was also suggested that activating PPAR $\beta/\delta$  in HaCaT keratinocytes promotes cell survival [15]. To determine whether over-expression of PPAR $\beta/\delta$  or PPAR $\gamma$  could modulate cell cycle progression, flow cytometric analysis was performed. Over-expression of PPAR $\beta/\delta$  in HaCaT keratinocytes caused a decrease in the percentage of cells at the G1 phase and an increase in the percentage of cells at the G2/M phase of the cell cycle as compared to control HaCaT keratinocytes (Fig. 4A). Over-expression of PPAR $\gamma$  in HaCaT keratinocytes caused a decrease in the percentage of cells in the G1 phase and the percentage of cells in S phase was increased as compared to control HaCaT keratinocytes (Fig. 4A). Ligand activation of PPAR $\beta/\delta$  with GW0742 (0.01–10.0  $\mu$ M) had no further effect on the distribution of cells in the different phases of the cell cycle in HaCaT keratinocytes, HaCaT-Migr1 vector control cells, and HaCaT-Migr1-hPPAR $\beta/\delta$  cells (Fig. 4B). Similarly, ligand activation of PPAR $\gamma$  with rosiglitazone (0.01–25.0  $\mu$ M) had no further effect on the distribution of cells in the different phases of the cell cycle in HaCaT keratinocytes, HaCaT-Migr1 vector control cells, and HaCaT-Migr1-hPPAR $\gamma$  cells (Fig. 4C, data not shown for 25  $\mu$ M).

#### 3.5. Effect of PPAR $\beta/\delta$ and PPAR $\gamma$ on induced apoptosis in HaCaT keratinocytes

While there is evidence that ligand activation of PPAR $\beta/\delta$  in HaCaT keratinocytes increases apoptosis [19], it was also suggested that activating PPAR $\beta/\delta$  in HaCaT keratinocytes promotes cell survival [15]. Further, docosahexaenoic acid, which can activate PPAR $\beta/\delta$  [22], can enhance UV-induced apoptosis in HaCaT keratinocytes [23]. Thus, the effect of staurosporine-induced or UVB-induced apoptosis was examined in HaCaT keratinocytes, HaCaT-Migr1 vector control cells, HaCaT-Migr1-hPPAR $\beta/\delta$  cells and HaCaT-Migr1-hPPAR $\gamma$  cells. Maximal PARP cleavage occurred by four hour post-staurosporine treatment in all four cells lines (Fig. 5A). Over-expression of PPAR $\beta/\delta$  or PPAR $\gamma$  in HaCaT keratinocytes had no effect on staurosporine-induced PARP cleavage (Fig. 5A). Ligand activation of PPAR $\beta/\delta$  with GW0742 (0.1 or 1.0  $\mu$ M) had no effect on staurosporine-induced PARP cleavage in either HaCaT keratinocytes, HaCaT-Migr1 vector control cells or HaCaT-Migr1-hPPAR $\beta/\delta$  cells (Fig. 5B). Moreover, ligand activation of PPAR $\gamma$  with rosiglitazone (1.0 or 10.0  $\mu$ M) did not influence staurosporine-induced PARP cleavage in either HaCaT keratinocytes, HaCaT-Migr1 vector control cells or HaCaT-Migr1-hPPAR $\gamma$  cells (Fig. 5C). Maximal

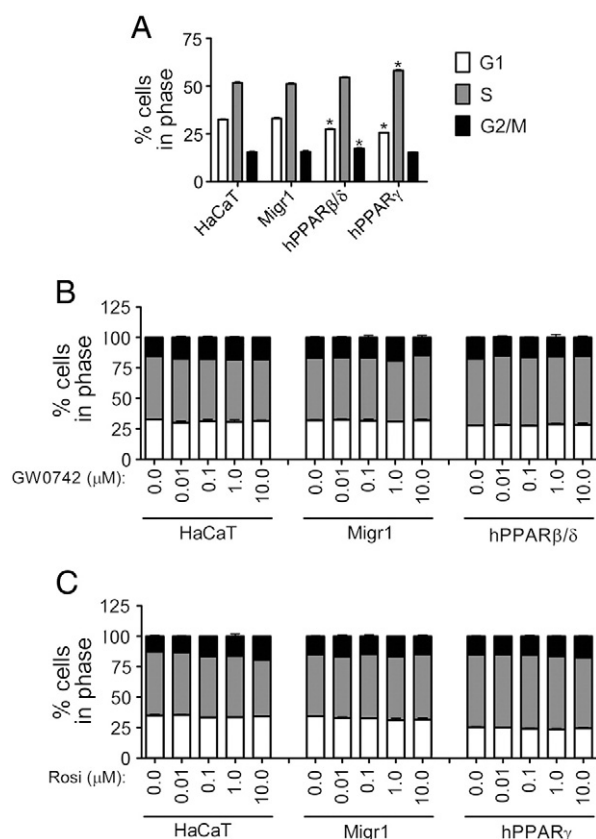


**Fig. 4.** Effect of over-expression of PPAR $\beta/\delta$  and PPAR $\gamma$  on cell cycle progression in HaCaT keratinocytes. Cell cycle progression was examined in HaCaT keratinocytes, HaCaT-Migr1 vector control cells (Migr1), HaCaT-Migr1-hPPAR $\beta/\delta$  cells (hPPAR $\beta/\delta$ ) and HaCaT-Migr1-hPPAR $\gamma$  cells (hPPAR $\gamma$ ) by flow cytometry. (A) Effect of over-expression of hPPAR $\beta/\delta$  or hPPAR $\gamma$  on cell cycle progression. (B) Effect of ligand activation of PPAR $\beta/\delta$  on cell cycle progression. Cells were treated for 24 h with 0.01–10  $\mu$ M GW0742. (C) Effect of ligand activation of PPAR $\gamma$  on cell cycle progression. Cells were treated for 24 h with 0.01–10  $\mu$ M rosiglitazone (Rosi). Values represent the mean  $\pm$  SEM, from three independent samples. \*Significantly different than control,  $P \leq 0.05$ .

PARP cleavage occurred by 8 hour post-UVB treatment in all four cells lines (Fig. 6A). UVB-induced PARP cleavage was not different between HaCaT keratinocytes, HaCaT-Migr1 vector control cells, HaCaT-Migr1-hPPAR $\beta/\delta$  cells or HaCaT-Migr1-hPPAR $\gamma$  cells (Fig. 6A). Ligand activation of PPAR $\beta/\delta$  with GW0742 (0.1 or 1.0  $\mu$ M) had no effect on UVB-induced PARP cleavage in either HaCaT keratinocytes, HaCaT-Migr1 vector control cells or HaCaT-Migr1-hPPAR $\beta/\delta$  cells (Fig. 6B). Similarly, ligand activation of PPAR $\gamma$  with rosiglitazone (1.0 or 10.0  $\mu$ M) did not influence UVB-induced PARP cleavage in either HaCaT keratinocytes, HaCaT-Migr1 vector control cells or HaCaT-Migr1-hPPAR $\gamma$  cells (Fig. 6C).

#### 3.6. Inhibition of UVB-induced expression of cytokines in HaCaT keratinocytes by PPAR $\beta/\delta$ and PPAR $\gamma$

Since PPAR $\beta/\delta$  and PPAR $\gamma$  can inhibit inflammatory signaling through both receptor-dependent and/or ligand-dependent mechanisms (reviewed in [3]), expression of mRNAs encoding inflammatory cytokines was examined in HaCaT keratinocytes, HaCaT-Migr1 vector control cells, HaCaT-Migr1-hPPAR $\beta/\delta$  cells and HaCaT-Migr1-hPPAR $\gamma$  cells. UVB-induced expression of *TNF $\alpha$* , *IL6* and *IL8* mRNA was markedly repressed in HaCaT-Migr1-hPPAR $\beta/\delta$  cells as compared to either HaCaT keratinocytes and/or HaCaT-Migr1 vector control cells (Fig. 7). Similar, but less striking repression of UVB-induced expression of these mRNAs encoding inflammatory cytokines in HaCaT-Migr1-hPPAR $\gamma$  cells as compared to HaCaT-Migr1 vector control cells was also observed (Fig. 7). These changes in mRNA expression were reflected by the concentrations of TNF $\alpha$  and IL6 in the culture medium (Fig. 7D,E).

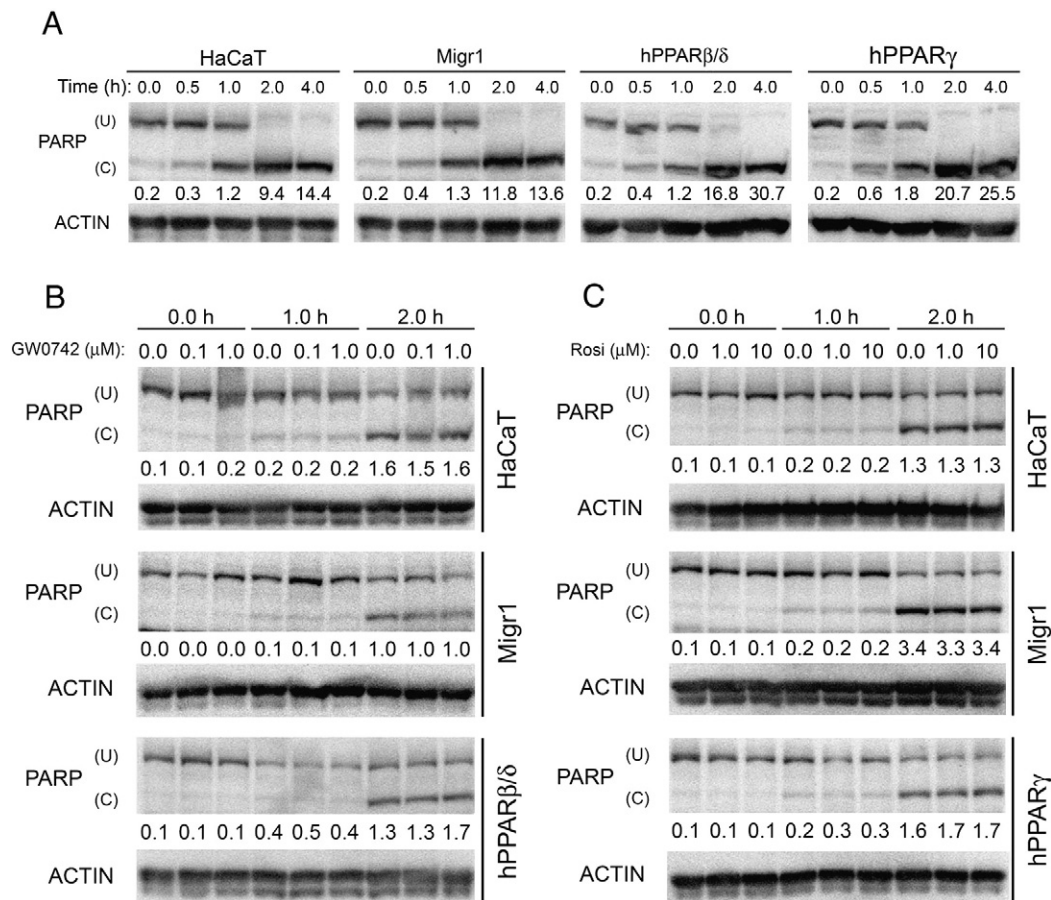


**Fig. 5.** Effect of over-expression and ligand activation of PPAR $\beta/\delta$  and PPAR $\gamma$  in HaCaT keratinocytes on staurosporine-induced PARP cleavage. (A) Quantitative Western blotting for PARP was performed using cell lysates from HaCaT keratinocytes, HaCaT-Migr1 vector control cells (Migr1), HaCaT-Migr1-hPPAR $\beta/\delta$  cells (hPPAR $\beta/\delta$ ) and HaCaT-Migr1-hPPAR $\gamma$  cells (hPPAR $\gamma$ ) treated with staurosporine (0.5  $\mu$ M) for the indicated times and quantitative Western blotting was performed. (B) Effect of ligand activation of PPAR $\beta/\delta$  on staurosporine-induced PARP cleavage. Cells were treated with GW0742 (0.1 or 1.0  $\mu$ M) for the indicated times and quantitative Western blotting was performed. (C) Effect of ligand activation of PPAR $\gamma$  on staurosporine-induced PARP cleavage. Cells were treated with rosiglitazone (1 or 10  $\mu$ M) for the indicated times and quantitative Western blotting was performed. (U) indicates uncleaved PARP and (C) indicates cleaved PARP. The ratio of C to U PARP was calculated and is presented below each sample.

Ligand activation of PPAR $\beta/\delta$  with GW0742 did not further repress the UVB-induced expression of *TNF $\alpha$* , *IL6* or *IL8* mRNA further than that found with PPAR $\beta/\delta$  over-expression alone (Fig. 8A–C). As compared to HaCaT-Migr1 vector control cells, UVB-induced expression of *TNF $\alpha$* , *IL6* or *IL8* mRNA was lower in HaCaT-Migr1-hPPAR $\gamma$  cells, but treatment with rosiglitazone did not further reduce expression (Fig. 8D–F).

#### 4. Discussion

Results from the present study establish the first stable, gain-of-function model for PPAR $\beta/\delta$  and PPAR $\gamma$  in HaCaT keratinocytes, a cell type where PPAR $\beta/\delta$  and PPAR $\gamma$  are known to play an important role in differentiation, cell proliferation and apoptosis [24] as reviewed in [5, 6, 8, 40]. The Migr1 retroviral system [14] is an ideal approach to over-express PPARs and isolate cell populations with high expression due to the ability to sort based on eGFP expression. Stable over-expression of PPAR $\beta/\delta$  and PPAR $\gamma$  resulted in HaCaT keratinocytes that exhibited markedly enhanced expression and function of these nuclear receptors. Thus, these cells will be useful for future studies to delineate the functional role of PPAR $\beta/\delta$  and PPAR $\gamma$  in human keratinocytes, and both complement and improve alternative approaches including the use of knockdown/knockout models and highly specific PPAR ligands.

Earlier studies suggested that PPAR $\beta/\delta$  might cross-talk with PPAR $\gamma$  [27,28]. For example, over-expression of PPAR $\beta/\delta$  in the monkey CV1 or COS1 cell lines represses PPAR $\gamma$  ligand-induced reporter activity [27,28]. Further, over-expression of PPAR $\beta/\delta$  in human NIH 3T3 cells represses PPAR $\gamma$  ligand-induced expression of PPAR $\gamma$ -dependent target gene

expression [25]. Thus, the present study examined this hypothetical cross-talk by comparing the effect of ligand activation of PPAR $\gamma$  in HaCaT keratinocytes over-expressing PPAR $\beta/\delta$ . In contrast to previous reports [27,28], PPAR $\gamma$  target gene expression was not repressed when expression of PPAR $\beta/\delta$  was markedly increased in HaCaT-Migr1-hPPAR $\beta/\delta$  cells. This suggests that over-expression of PPAR $\beta/\delta$  does not interfere with PPAR $\gamma$ -dependent transcription. This is consistent with the observation that PPAR $\gamma$  ligand-induced expression of PPAR $\gamma$  target genes required for adipocyte differentiation is not enhanced in *Ppar $\beta/\delta$* -null adipocytes [26]. In fact, in this model, expression of PPAR $\beta/\delta$  potentiated PPAR $\gamma$ -dependent adipocyte differentiation [26], suggesting that PPAR $\beta/\delta$  alters ligand-dependent function of PPAR $\gamma$  through an additive mechanism. The finding from the present work that PPAR $\beta/\delta$  does not interfere with PPAR $\gamma$ -dependent transcription is also consistent with previous *in vivo* analysis of *Ppar $\beta/\delta$* -null mice where ligand activation of PPAR $\gamma$  in *Ppar $\beta/\delta$* -null mouse colon (a tissue known to express PPAR $\beta/\delta$  and PPAR $\gamma$  at very high levels [42, 43]) does not lead to enhanced expression of PPAR $\gamma$  target genes [27]. These observations suggest that physiologically, it is unlikely that PPAR $\beta/\delta$  interferes with PPAR $\gamma$  transcription as suggested by *in vitro* studies. Since previous studies suggesting that PPAR $\beta/\delta$  interferes with PPAR $\gamma$  transcription based this interpretation in part on data from reporter constructs [27,28], it remains a possibility that the observed differences were due to receptor-dependent modulation of transcriptional events observed with plasmid constructs that lack chromatin structure associated with endogenous target genes. Another possible explanation for the differences between the present study showing no change in PPAR $\gamma$  target gene expression when



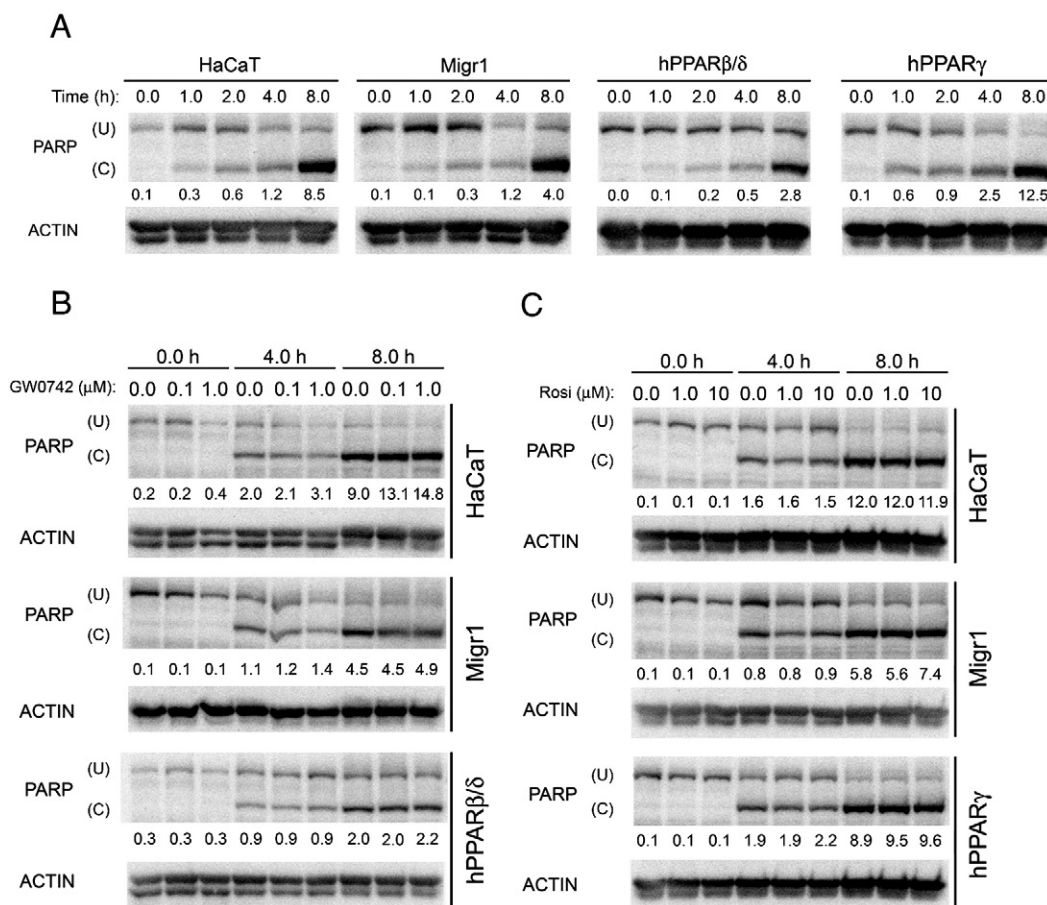


**Fig. 6.** Effect of over-expression and ligand activation of PPAR $\beta/\delta$  and PPAR $\gamma$  in HaCaT keratinocytes on UVB-induced PARP cleavage. (A) Quantitative Western blotting for PARP was performed using cell lysates from HaCaT keratinocytes, HaCaT-Migr1 vector control cells (Migr1), HaCaT-Migr1-hPPAR $\beta/\delta$  cells (hPPAR $\beta/\delta$ ) and HaCaT-Migr1-hPPAR $\gamma$  cells (hPPAR $\gamma$ ) irradiated with UVB for the indicated times. (B) Effect of ligand activation of PPAR $\beta/\delta$  on UVB-induced PARP cleavage. Cells were treated with GW0742 (0.1 or 1.0  $\mu$ M) for the indicated times and quantitative Western blotting was performed. (C) Effect of ligand activation of PPAR $\gamma$  on UVB-induced PARP cleavage. Cells were treated with rosiglitazone (1 or 10  $\mu$ M) for the indicated times and quantitative Western blotting was performed. (U) indicates uncleaved PARP and (C) indicates cleaved PARP. The ratio of C to U PARP was calculated and is presented below each sample.

PPAR $\beta/\delta$  is over-expressed, and others showing inhibition of PPAR $\gamma$  target gene expression when PPAR $\beta/\delta$  is over-expressed, is that over-expression of PPAR $\beta/\delta$  could deplete co-effectors required by PPAR $\gamma$  for transcription (e.g. co-activators) in COS1 or CV1 cells while this does not occur in HaCaT keratinocytes. It is thus important to note that the level of over-expression of PPAR $\beta/\delta$  in these models may not reflect physiological achievable concentrations. If this is true, then the observed inhibition of PPAR $\gamma$ -dependent transcription may be an artifact of the in vitro model that does not model normal physiology. This idea is supported by the in vivo analysis showing that disruption of expression of PPAR $\beta/\delta$  in tissues that express very high levels of both PPAR $\beta/\delta$  and PPAR $\gamma$  does not alter PPAR $\gamma$  ligand inducibility of PPAR $\gamma$  target gene expression [26].

The hypothetical signaling proposed by others suggesting that the biological effects of atRA can be modulated by differential shuttling between RAR and PPAR $\beta/\delta$  [15] based on the expression of FABP5 and CRABP-II led to the examination of this signaling in HaCaT keratinocytes in the present study. HaCaT keratinocytes are ideal for this purpose because they express high levels of FABP5 as compared to CRABP-II, and HaCaT is the same cell line used to suggest this hypothetical signaling [15]. As noted above, the potency of ligand activation and efficacy of PPAR $\beta/\delta$  target expression was enhanced in HaCaT keratinocytes over-expressing PPAR $\beta/\delta$  in response to a highly specific PPAR $\beta/\delta$  ligand. However, despite the fact that atRA was capable of activating RAR in control HaCaT keratinocytes, HaCaT-Migr1 vector control cells, and HaCaT-Migr1-hPPAR $\beta/\delta$  cells (as shown by increased expression of CYP26A1), no evidence of enhanced shuttling of atRA towards activating PPAR $\beta/\delta$  and increasing PPAR $\beta/\delta$  target gene expression was observed.

These results are consistent with previous studies showing that: 1) atRA does not increase *Angptl4* mRNA expression in HaCaT keratinocytes or mouse keratinocytes [19], 2) atRA does not cause PPAR $\beta/\delta$ -dependent anti-apoptotic activities in mouse keratinocytes [19], 3) atRA does not cause an increase in PPAR $\beta/\delta$ -dependent reporter assays [28], and 4) atRA does not cause association of PPAR $\beta/\delta$  with co-activators based on a time-resolved fluorescence resonance energy transfer assay [28]. The present studies advance the former findings because even when expression of PPAR $\beta/\delta$  is markedly increased in HaCaT keratinocytes where the FABP5:CRABP-II is high, atRA does not activate PPAR $\beta/\delta$ ; moreover, atRA or GW0742 do not increase expression of PDK1, and GW0742 does not attenuate UVB-induced PARP cleavage. Collectively, these observations and results from the present study demonstrate that no shuttling of atRA toward activating PPAR $\beta/\delta$  occurs in cells expressing high levels of FABP5 as compared to CRABP-II, even when PPAR $\beta/\delta$  expression is markedly increased. This reinforces the notion that the hypothesis that the biological effects of atRA can be modulated by differential shuttling between RAR and PPAR $\beta/\delta$  based on the expression of FABP5 and CRABP-II [15], should be rigorously re-examined.

Inhibition of HaCaT cell proliferation is found in response to ligand activation of PPAR $\beta/\delta$ , but these changes are modest and only occur after 72 h of treatment [19]. Over-expression of PPAR $\beta/\delta$  in HaCaT keratinocytes did not markedly alter cell cycle progression as compared to controls, but a decrease in the percentage of cells in the G1 phase and an increase in the percentage of cells at the G2/M phase was noted; an effect that was not further influenced by ligand activation of PPAR $\beta/\delta$ . This is in contrast to results observed in N/TERT-1 keratinocytes where

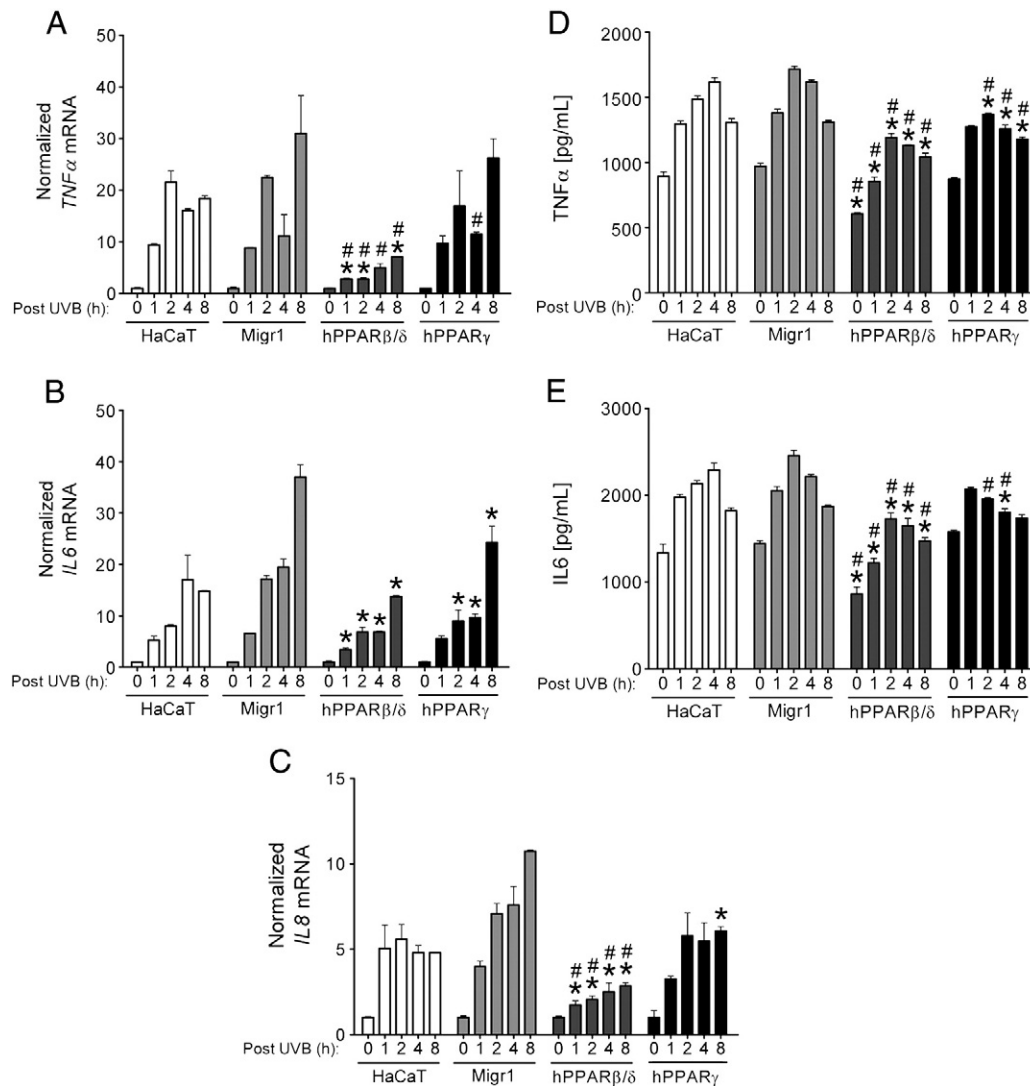


**Fig. 7.** Effect of over-expression of PPAR $\beta/\delta$  and PPAR $\gamma$  in HaCaT keratinocytes on UVB-induced expression and secretion of inflammatory cytokines. HaCaT keratinocytes, HaCaT-Migr1 vector control cells (Migr1), HaCaT-Migr1-hPPAR $\beta/\delta$  cells (hPPAR $\beta/\delta$ ) and HaCaT-Migr1-hPPAR $\gamma$  cells (hPPAR $\gamma$ ) were irradiated with UVB for the indicated times and mRNA expression of the inflammatory cytokines (A) *TNF $\alpha$* , (B) *IL6*, and (C) *IL8*, or the concentration of culture medium (D) *TNF $\alpha$*  and (E) *IL6*, was examined. Fold induction of cytokine mRNA was calculated by normalization to the non-UVB control for each cell line. Data represents triplicate independent sample means  $\pm$  SEM. \*statistically different as compared to the HaCaT-Migr1 vector control cell line by Student's *T*-test at each time point ( $P < 0.05$ ). #statistically different compared to the HaCaT keratinocytes by Student's *T*-test at each time point ( $P < 0.05$ ).

ligand activation of PPAR $\beta/\delta$  inhibits cell cycle progression by increasing the percentage of cells in the G1 phase and decreasing the percentage of cells in S phase [29]. The reason why an increase in the percentage of cells in the G2/M phase and a decrease in the percentage of cells in the G1 phase of the cell cycle was found in HaCaT-Migr1-hPPAR $\beta/\delta$  keratinocytes while an increase in the percentage of cell in the G1 phase of the cell cycle was found in N/TERT-1 keratinocytes cannot be determined from these studies. However, this could be due in part to differences in the genetic alterations causing immortalization of HaCaT (p53) and N/TERT-1 keratinocytes (hTERT), or the fact that HaCaT keratinocytes are resistant to induced growth inhibition [21,30,31].

Over-expression of PPAR $\gamma$  also caused a decrease in the percentage of cells in the G1 phase of the cell cycle, but this change was associated with an increase in the percentage of cells in S phase of the cells cycle. Ligand activation of PPAR $\gamma$  did not further influence these kinetics. Previous studies have shown that activating PPAR $\gamma$  in mouse and human keratinocytes can inhibit cell proliferation [36, 37, 49]. Results from the present studies are inconsistent with these studies, but could also be influenced by the relative resistance to growth inhibition observed in HaCaT keratinocytes [21]. However, it is of

interest to note that expression of PPAR $\gamma$  is increased during the resolution phase of wound healing [32], during which a transition between active cell proliferation and apoptosis is observed. Thus, the finding that over-expression of PPAR $\gamma$  in HaCaT keratinocytes caused a modest increase in the percentage of cells in the S phase of the cell cycle may reflect this model. Further studies with the HaCaT-Migr1-hPPAR $\gamma$  keratinocytes may be suitable to examine this in greater detail. Alternatively, the increase in the percentage of cells in the S phase resulting from over-expression of PPAR $\gamma$  could be influenced by the mutant p53 gene in HaCaT keratinocytes [31].

Ligand activation of PPAR $\beta/\delta$  in HaCaT keratinocytes can modestly increase apoptosis [19], but it was also suggested that activating PPAR $\beta/\delta$  in HaCaT keratinocytes promotes cell survival [15]. Results from the present studies demonstrate that over-expression of PPAR $\beta/\delta$  or PPAR $\gamma$  did not markedly alter PARP cleavage induced by either staurosporine or UVB. Further, ligand activation of either PPAR $\beta/\delta$  or PPAR $\gamma$ , in the presence or absence of over-expressed receptor, did not influence either staurosporine- or UVB-induced PARP cleavage. These results are in contrast to studies suggesting that activating PPAR $\beta/\delta$  causes decreased expression of PTEN, increased

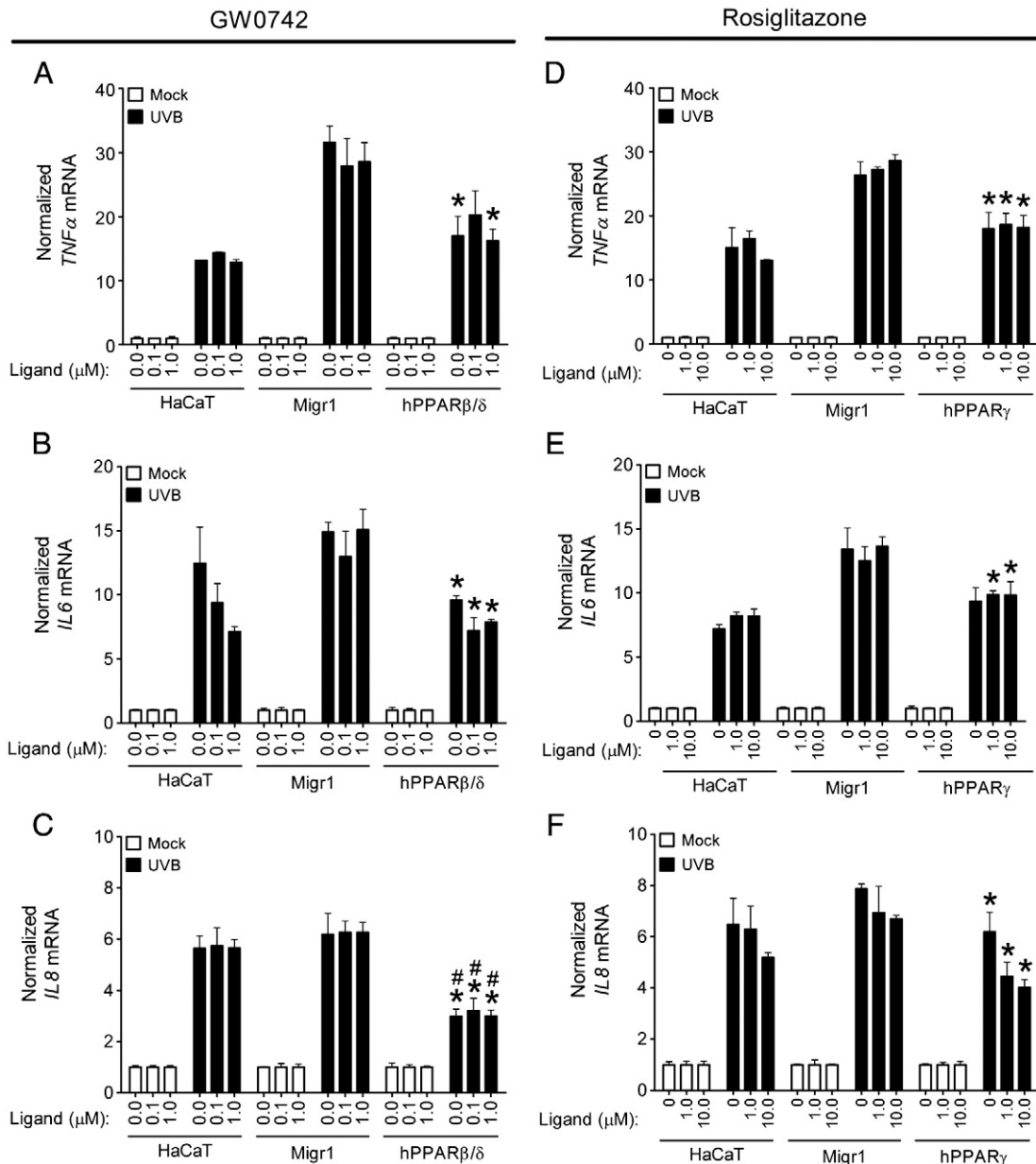


**Fig. 8.** Effect of ligand activation of PPAR $\beta/\delta$  and PPAR $\gamma$  on UVB-induced expression of inflammatory cytokines in HaCaT keratinocytes over-expressing of PPAR $\beta/\delta$  and PPAR $\gamma$ . HaCaT keratinocytes, HaCaT-Migr1 vector control cells (Migr1), HaCaT-Migr1-hPPAR $\beta/\delta$  cells (hPPAR $\beta/\delta$ ) and HaCaT-Migr1-hPPAR $\gamma$  cells (hPPAR $\gamma$ ) were treated with either 0, 0.1 or 1.0  $\mu$ M GW0742, or 0, 1 or 10  $\mu$ M rosiglitazone and irradiated with UVB, and mRNA expression of the inflammatory cytokines (A,D) *TNF $\alpha$* , (B,E) *IL6*, and (C,F) *IL8* was examined 4 hour post-UVB treatment. Fold induction of cytokine mRNA was calculated by normalization to the non-UVB control for each cell line. Data represents triplicate independent sample means  $\pm$  SEM. \*statistically different as compared to the HaCaT-Migr1 vector control cell line by Student's *T*-test at each time point ( $P < 0.05$ ). #statistically different compared to the HaCaT keratinocytes by Student's *T*-test at each time point ( $P < 0.05$ ).

expression of ILK and PDPK1 causing phosphorylation of AKT and enhanced cell survival in HaCaT keratinocytes [33]. If activating PPAR $\beta/\delta$  caused anti-apoptotic activity, then reduced PARP cleavage would be expected, and this was not found in the present study. These results are however consistent with a recent study showing that ligand activation of PPAR $\beta/\delta$  did not prevent non-steroidal anti-inflammatory drug (NSAID)-induced apoptosis or increase the number of viable cells in human colon cancer cells [34]. Moreover, the lack of change in PDPK1 expression following ligand activation of PPAR $\beta/\delta$  in the presence or absence of over-expressed PPAR $\beta/\delta$  in HaCaT keratinocytes is also consistent with other studies where no change in expression of PTEN, PDPK1, ILK and/or phosphorylated AKT were found in mouse keratinocytes, N/TERT-1 keratinocytes or HaCaT keratinocytes [30, 54]. Collectively, these results demonstrate that activating PPAR $\beta/\delta$ , with or without over-expression of PPAR $\beta/\delta$

in HaCaT keratinocytes does not prevent staurosporine- or UVB-induced apoptosis.

Expression of inflammatory cytokine expression was also examined in HaCaT keratinocytes because PPAR $\beta/\delta$  and PPAR $\gamma$  can inhibit inflammatory signaling through both receptor-dependent and/or ligand-dependent mechanisms (reviewed in [3]). Over-expression of PPAR $\beta/\delta$  or PPAR $\gamma$  both reduced UVB-induced mRNA expression of *TNF $\alpha$* , *IL6* and *IL8*, but this effect was more striking in cells over-expressing PPAR $\beta/\delta$ . Consistent with these observations, UVB-induced secretion of *TNF $\alpha$*  and *IL6* was also repressed in cells over-expressing PPAR $\beta/\delta$  or PPAR $\gamma$ . Ligand activation of either PPAR $\beta/\delta$  or PPAR $\gamma$  did not modulate the receptor-dependent repression of UVB-induced expression of *TNF $\alpha$* , *IL6* or *IL8* mRNA. This observation is similar to PPAR $\beta/\delta$ -dependent repression of dextran sodium sulfate (DSS)-induced colitis where DSS-induced colitis is exacerbated in

*Pparβ/δ*-null mice as compared to wild-type mice, but ligand activation of PPARβ/δ did not further influence DSS-induced colitis [35]. Since receptor-dependent repression of UVB-induced expression of inflammatory cytokines in HaCaT keratinocytes is not influenced by exogenous ligands, it remains possible that high affinity endogenous ligands prevent any further modulation due to differences in relative receptor affinity. It is also possible that PPAR-dependent repression of UVB-induced expression of inflammatory cytokines does not require ligand activation and is mediated through mechanisms facilitated by PPARs interacting with other transcription factors such as the p65 subunit of NF-κB thereby attenuating NF-κB-dependent signaling. Further studies are needed to examine this hypothesis and the HaCaT-Migr1-hPPARβ/δ and the HaCaT-Migr1-hPPARγ keratinocytes are excellent models for this purpose.

In conclusion, results from the present study demonstrate the feasibility of the Migr1 system to over-express PPARs in HaCaT keratinocytes in order to generate a model to delineate the functional roles of PPARs in these cells. This approach is likely suitable for other cell lines as well. These models will complement knockout and knockdown approaches and provide an alternative approach to determine receptor-dependent and ligand-dependent function of receptors with great promise for therapeutic targets.

Author contributions: MB designed and performed the experiments, interpreted the data and wrote the manuscript. CK performed experiments and reviewed the manuscript. PPA helped make the Migr1-hPPARβ/δ construct, performed experiments and reviewed the manuscript. BZ helped make the Migr1-hPPARβ/δ and Migr1-hPPARγ construct and reviewed the manuscript. TSL helped make the Migr1-hPPARγ construct and reviewed the manuscript. CL performed experiments and reviewed the manuscript. FJG and JMP designed experiments, interpreted the data and wrote the manuscript.

## Acknowledgments

We gratefully acknowledge Drs. Andrew N. Billin and Timothy M. Willson for providing GW0742, Dr. Gary H. Perdew for the use of a fluorescent microscope, and Susan Magargee and Nicole Bem from the Center for Quantitative Cell Analysis at the Huck Institutes of Life Sciences of The Pennsylvania State University for their technical support in sorting the fluorescent cells. This work was supported in part by the National Institutes of Health Grants CA124533, CA126826, CA141029, CA140369 (JMP) and the National Cancer Institute Intramural Research Program ZIABC005561, ZIABC005562, ZIABC005708 (FJG).

## References

[1] T. Tanaka, J. Yamamoto, S. Iwasaki, H. Asaba, H. Hamura, Y. Ikeda, M. Watanabe, K. Magoori, R.X. Ioka, K. Tachibana, Y. Watanabe, Y. Uchiyama, K. Sumi, H. Iguchi, S. Ito, T. Doi, T. Hamakubo, M. Naito, J. Auwerx, M. Yanagisawa, T. Kodama, J. Sakai, *Proc. Natl. Acad. Sci. U. S. A.* 100 (26) (2003) 15924–15929.  
 [2] W.R. Oliver Jr., J.L. Shenk, M.R. Snaith, C.S. Russell, K.D. Plunket, N.L. Bodkin, M.C. Lewis, D.A. Winegar, M.L. Sznajdman, M.H. Lambert, H.E. Xu, D.D. Sternbach, S.A. Klierer, B.C. Hansen, T.M. Willson, *PNAS* (2001) 5306–5311.

[3] K.S. Kilgore, A.N. Billin, *Curr. Opin. Investig. Drugs* 9 (5) (2008) 463–469.  
 [4] M.A. Peraza, A.D. Burdick, H.E. Marin, F.J. Gonzalez, J.M. Peters, *Toxicol. Sci.* 90 (2) (2006) 269–295.  
 [5] J.M. Peters, F.J. Gonzalez, *Biochim. Biophys. Acta* 1796 (2) (2009) 230–241.  
 [6] P.S. Palkar, M.G. Borland, S. Naruhn, C.H. Ferry, C. Lee, U.H. Sk, A.K. Sharma, S. Amin, I.A. Murray, C.R. Anderson, G.H. Perdew, F.J. Gonzalez, R. Muller, J.M. Peters, *Mol. Pharmacol.* (2010), doi:10.1124/mol.110.065508.  
 [7] E.E. Giroir, H.E. Hollingshead, P. He, B. Zhu, G.H. Perdew, J.M. Peters, *Biochem. Biophys. Res. Commun.* 371 (3) (2008) 456–461.  
 [8] L. Berglund, E. Bjorling, P. Oksvold, L. Fagerberg, A. Asplund, C.A. Szgyarto, A. Persson, J. Ottosson, H. Wernerus, P. Nilsson, E. Lundberg, A. Sivertsson, S. Navani, K. Wester, C. Kampf, S. Hober, F. Ponten, M. Uhlen, *Mol. Cell. Proteomics* 7 (10) (2008) 2019–2027.  
 [9] D.J. Kim, T.E. Akiyama, F.S. Harman, A.M. Burns, W. Shan, J.M. Ward, M.J. Kennett, F.J. Gonzalez, J.M. Peters, *J. Biol. Chem.* 279 (22) (2004) 23719–23727.  
 [10] Y. Barak, D. Liao, W. He, E.S. Ong, M.C. Nelson, J.M. Olefsky, R. Boland, R.M. Evans, *PNAS* 99 (1) (2002) 303–308.  
 [11] D. Wang, H. Wang, Y. Guo, W. Ning, S. Katkuri, W. Wahli, B. Desvergne, S.K. Dey, R.N. Dubois, *Proc. Natl. Acad. Sci. U. S. A.* 103 (50) (2006) 19069–19074.  
 [12] B.G. Shearer, W.J. Hoekstra, *Curr. Med. Chem.* 10 (4) (2003) 267–280.  
 [13] M.L. Sznajdman, C.D. Haffner, P.R. Maloney, A. Fivush, E. Chao, D. Goreham, M.L. Sierra, C. LeGrumelec, H.E. Xu, V.G. Montana, M.H. Lambert, T.M. Willson, W.R. Oliver, D.D. Sternbach, *Bioorg. Med. Chem. Lett.* 13 (9) (2003) 1517–1521.  
 [14] W.S. Pear, J.P. Miller, L. Xu, J.C. Pui, B. Soffer, R.C. Quackenbush, A.M. Pendergast, R. Bronson, J.C. Aster, M.L. Scott, D. Baltimore, *Blood* 92 (10) (1998) 3780–3792.  
 [15] T.T. Schug, D.C. Berry, N.S. Shaw, S.N. Travis, N. Noy, *Cell* 129 (4) (2007) 723–733.  
 [16] A. Chawla, C.H. Lee, Y. Barak, W. He, J. Rosenfeld, D. Liao, J. Han, H. Kang, R.M. Evans, *PNAS* 100 (3) (2003) 1268–1273.  
 [17] R.A. Gupta, J.A. Brockman, P. Sarraf, T.M. Willson, R.N. DuBois, *J. Biol. Chem.* 276 (32) (2001) 29681–29687.  
 [18] S. Mandar, J.E. Foreman, N.S. Tan, P. Escher, D. Patsouris, W. Koenig, R. Kleemann, A. Bakker, F. Veenman, W. Wahli, M. Muller, S. Kersten, *J. Biol. Chem.* 279 (33) (2004) 34411–34420.  
 [19] M.G. Borland, J.E. Foreman, E.E. Giroir, R. Zolfaghari, A.K. Sharma, S. Amin, F.J. Gonzalez, A.C. Ross, J.M. Peters, *Mol. Pharmacol.* 74 (5) (2008) 1429–1442.  
 [20] M. Westergaard, J. Henningsen, M.L. Svendsen, C. Johansen, U.B. Jensen, H.D. Schroder, I. Kratchmarova, R.K. Berge, L. Iversen, L. Bolund, K. Kragballe, K. Kristiansen, *J. Invest. Dermatol.* 116 (5) (2001) 702–712.  
 [21] U. Henseleit, T. Rosenbach, G. Kolde, *Arch. Dermatol. Res.* 288 (11) (1996) 676–683.  
 [22] B.M. Forman, J. Chen, R.M. Evans, *PNAS* 94 (9) (1997) 4312–4317.  
 [23] S. Serini, V. Donato, E. Piccioni, S. Trombino, G. Monego, A. Toesca, I. Innocenti, M. Missori, M. De Spirito, L. Celleno, E. Fasano, F.O. Ranelletti, G. Calviello, J. Nutr. *Biochem.* (2011), doi:10.1016/j.nutbio.2010.08.004.  
 [24] C.N. Ellis, J. Varani, G.J. Fisher, M.E. Zeigler, H.A. Pershadsingh, S.C. Benson, Y. Chi, T.W. Kurtz, *Arch. Derm.* 136 (5) (2000) 609–616.  
 [25] Y. Shi, M. Hon, R.M. Evans, *PNAS* 99 (5) (2002) 2613–2618.  
 [26] K. Matsusue, J.M. Peters, F.J. Gonzalez, *FASEB J.* (2004) 04-1944fje.  
 [27] H.E. Marin, M.A. Peraza, A.N. Billin, T.M. Willson, J.M. Ward, M.J. Kennett, F.J. Gonzalez, J.M. Peters, *Cancer Res.* 66 (8) (2006) 4394–4401.  
 [28] M. Rieck, W. Meissner, S. Ries, S. Muller-Brusselbach, R. Muller, *Mol. Pharmacol.* 74 (5) (2008) 1269–1277.  
 [29] A.D. Burdick, M.T. Bility, E.E. Giroir, A.N. Billin, T.M. Willson, F.J. Gonzalez, J.M. Peters, *Cell. Signal.* 19 (6) (2007) 1163–1171.  
 [30] M.A. Dickson, F.C. Hahn, Y. Ino, V. Ronfard, J.Y. Wu, R.A. Weinberg, D.N. Louis, F.P. Li, J.G. Rheinwald, *Mol. Cell. Biol.* 20 (4) (2000) 1436–1447.  
 [31] T.A. Lehman, R. Modali, P. Boukamp, J. Stanek, W.P. Bennett, J.A. Welsh, R.A. Metcalf, M.R. Stampfer, N. Fusenig, E.M. Rogan, et al., *Carcinogenesis* 14 (5) (1993) 833–839.  
 [32] M. Kapoor, F. Kojima, L. Yang, L.J. Crofford, *Prostaglandins Leukot. Essent. Fatty Acids* 76 (2) (2007) 103–112.  
 [33] N. Di-Poi, N.S. Tan, L. Michalik, W. Wahli, B. Desvergne, *Mol. Cell* 10 (4) (2002) 721–733.  
 [34] J.E. Foreman, W.-C. Chang, P.S. Palkar, B. Zhu, M.G. Borland, J.L. Williams, L.R. Kramer, M.L. Clapper, F.J. Gonzalez, J.M. Peters, *Mol. Carcinog.* (2011), doi:10.1002/mc.20757.  
 [35] H.E. Hollingshead, K. Morimura, M. Adachi, M.J. Kennett, A.N. Billin, T.M. Willson, F.J. Gonzalez, J.M. Peters, *Dig. Dis. Sci.* 52 (11) (2007) 2912–2919.